Interpolation based "time of travel" scheme in a Visual Motion Sensor using a small 2D retina

Fabien Expert, Frédéric L. Roubieu, Franck Ruffier

Interpolation based "time of travel" scheme in a Visual Motion Sensor using a small 2D retina.

Fabien Expert, Frédéric L. Roubieu, Franck Ruffier
Aix-Marseille University, CNRS, ISM UMR 7287, Biorobotics dept., 13288, Marseille, France
{fabien.expert, frederic.roubieu, franck.ruffier} @univ-amu.fr

***Abstract*—Insects flying abilities based on optic flow (OF) are nice bio-inspired models for Micro Aerial Vehicles (MAVs) endowed with a limited computational power. Most OF sensing robots developed so far have used numerically complex algorithms requiring large computational power often carried out offline. The present study shows the performances of our bio-inspired Visual Motion Sensor (VMS) based on a 3x4 matrix of auto-adaptive aVLSI photoreceptors pertaining to a custom-made bio-inspired chip called APIS (Adaptive Pixels for Insect-based Sensors). To achieve such processing with the limited computational power of a tiny microcontroller (µC), the µC-based implementation of the "time of travel" scheme requiring at least a 1kHz sampling rate was modified by linearly interpolating the photoreceptors signals to run the algorithm at a lower sampling rate. The accuracy of the measurements was assessed for various sampling rates in simulation and the best trade-off between computational load and accuracy determined at 200Hz was implemented onboard a tiny µC. By interpolating the photoreceptors signals and by fusing the output of several Local Motion Sensors (LMSs), we ended up with an accurate and frequently refreshed VMS measuring a visual angular speed and requiring more than 4 times less computational resources.**

***Index Terms*—Elementary Motion Detector, EMD, Optic flow, Insect Vision, Micro-aerial vehicle (MAV), bio-inspiration.**

I. Introduction

Despite their small size, airborne insects such as flies and bees can navigate autonomously in unknown environments on the basis of Optic Flow (OF) cues. Several bio-inspired terrestrial and aerial robots have been developed during the past decade based on similar principles [8], [17], [2]. However, the computation of the OF onboard Micro Aerial Vehicles (MAVs) is still a challenging task, as most OF algorithms require a heavy computational load [14], [13] conflicting with their limited payload. Several methods of measuring the visual angular speed requiring few computational resources have been developed, such as those involving the local 1-D Hassenstein-Reichardt correlator [12], which was mounted on a terrestrial robot [11]; the Interpolation Image Algorithm (I2A) [19] which was used onboard an indoor microflyer [21] and the "time of travel" scheme [3], [18] originally inspired by the fly's Elementary Motion Detector (EMD) neurons [9].

Recently, we focused on developing lightweight OF sensors embedded into tiny µC [18], [15], [20], [7] based on this scheme. In a previous study, we showed how 5 Local Motion Sensors (LMSs) measuring the angular speed (i.e., a 1-D component of the OF) can be embedded into a small µC to robustly and accurately determine the angular speed using the median operator [16]. Nevertheless, we were limited to implement more LMSs inside the same µC by the high sampling rate (at least 1kHz) that was necessary to determine accurately the time-lag Δt between two adjacent visual signals. In this study, we show that a linear interpolation of the visual signals acquired at lower sampling rates can also result in an accurate angular speed measurement at a lower cost in terms of computational load and therefore allow to increase the number of LMS implemented into a single µC. The performances of this optimized implementation have been tested on a 3x4 matrix of Delbrück-type auto-adaptive aVLSI pixels [5] pertaining to a custom-made bio-inspired chip called APIS (Adaptive Pixels for Insect-based Sensors) [1], [20] in front of a moving wall lined with a natural panorama (see Fig. 1).

Section 2 gives a short description of the bio-inspired visual system and optimized implementation of the "time of travel" scheme. Section 3 describes the experiments and the results obtained with the Visual Motion Sensor (VMS), which was tested indoors under natural light conditions.

II. Optimized implementation

Each LMS assesses the angular speed ω_i of any contrasting object detected by 2 neighboring photosensor signals thanks to the *new interpolation based "time of travel" scheme* which can now be described in 7 processing steps including the new Interpolation Step n°5 (see Fig. 2a):

- Step 1: Low-pass spatial filtering is achieved by defocusing the lens, thus giving each pixel in the array a Gaussian angular sensitivity function define by an inter-receptor angle $\Delta\varphi = 3.8^o$ and an acceptance angle $\Delta\rho = 3.8^o$.
- Step 2: Analog low-pass anti-aliasing filtering $f_c = 50Hz$.
- Step 3: Digitizing and filtering: second order fixed-point digital low-pass filtering ($f_c = 30Hz$) reduces any high frequency noise introduced by the artificial indoor lighting (100Hz) and first order fixed-point high-pass filtering ($f_c = 10Hz$).
- Step 4: Hysteresis thresholding is performed to distinguish between 'ON' and 'OFF' contrast transitions (i.e. dark-to-light and light-to-dark transitions, respectively) in each channel.
- Step 5: Linear interpolation of the photoreceptor signals acquired at a frequency f_{sample} to improve the temporal resolution of the angular speed computation. As shown in Fig. 2b, each time a signal exceeds a threshold, the

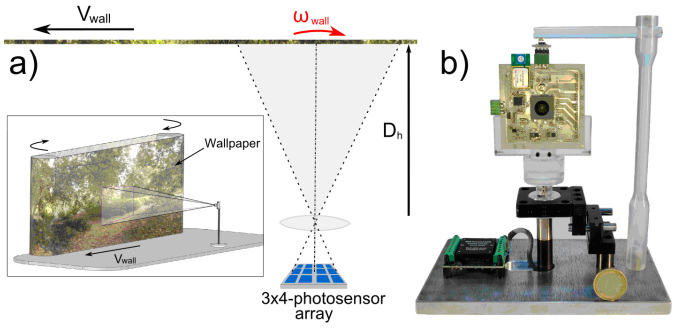

Figure 1. a) Test-bed for testing the visual motion device including the 3x4-photosensor array placed at an orthogonal distance D_h from a wall lined with a natural pattern moving at a speed V_{wall}. b) Picture of the test-board used for the experiments with the 25 auto-adaptive pixel array covered by its lens (Sparkfun SEN-00637, focal length 2mm, f-number 2.8) in the center. Each pixel features an integrated photodiode with a sensitive area of $250 \times 250 \mu m$ connected to an adaptive, time-continuous, logarithmic circuit having a dynamic range of 100 dB.

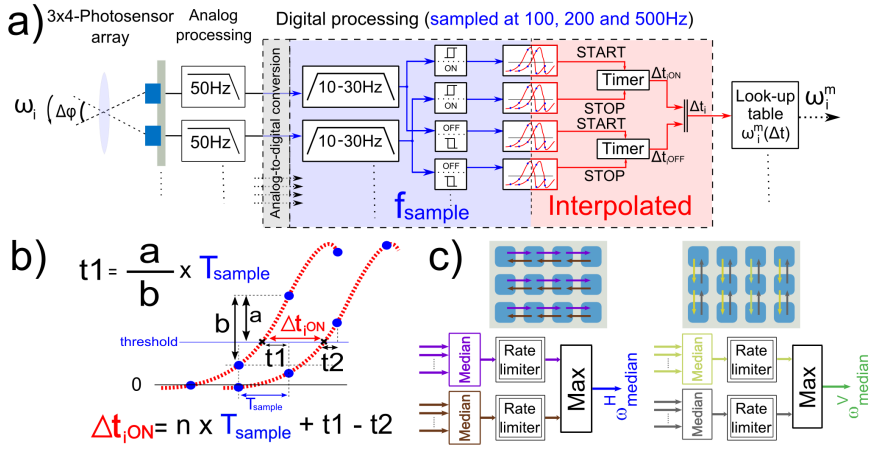

Figure 2. a) General processing architecture of the Local Motion Sensor (LMS): the output signals of two adjacent pixels were spatially and temporally filtered and thresholded to determine each 2-pixel angular speed ω_i^m. The data acquired at f_{sample} were linearly interpolated to measure the time-lag Δt between the two signals. b) Linear interpolation method to increase the resolution of the time difference measured between the signals of two adjacent pixels. Every time both visual signal exceed the positive threshold, the times (t1 and t2) are computed to estimate the interpolated Δt_{iON}, in this case. c) Fusion algorithm based on the maximal median value of both directions [4], [8] used to determine the magnitude and the direction of the 1-D angular speeds ω^H_{median} and ω^V_{median}. A rate limiter function filters out any median angular speed measurements that change too fast.

time delays $t1$ or $t2$ are estimated with a 2kHz resolution assuming a linear variation of the signal between two samples.

- Step 6: A time delay circuit is triggered by one channel and stopped by the neighboring channel. This function measures the delay $\Delta t_i = n \times T_{sample} + t_1 - t_2$ elapsing between similar ('ON' or 'OFF') transitions occurring in two adjacent photoreceptors.
- Step 7: Computing the 1-D angular speed within the visual field of the LMS by using a look-up table that transforms the delay into the measured angular speed ω_i^m by applying $\omega_i^m = \frac{\triangle \varphi}{\Delta t_i}$.

III. Experiment and Results

The visual motion sensor was tested indoors with natural light at an illuminance of around $0.7 \times 10^{-3} W/cm^2$ corresponding to the daylight provided by a window. The VMS was placed at an orthogonal distance $D_h = 27.5cm$ from a printed strip of wallpaper depicting a natural colored scene (see Fig. 1a) and could be rotated by an angle of 90^o. The printed strip was stretched between 2 actuated drums imposing a translational speed V_{wall} to the panorama. The scene was therefore seen to move horizontally or vertically by the VMS at an angular speed ω_{wall} describing a triangular speed law involving a series of velocity ramps with different slopes ranging between $75^o/s$ and $275^o/s$.

Among the 25 pixels of the APIS retina, a 4x3-pixel array is connected to the microcontroller and 34 LMSs are computed (represented by the arrows in Fig. 2c) in 4 different directions (from top to bottom, from bottom to top, from left to right and from right to left). In each direction, the median value of the angular speed is computed and the maximum value between the median value of opposite directions determines respectively ω^H_{median} and ω^V_{median} .

The data dispersion was taken to be the standard deviation of the difference between the theoretical angular speed determined from the horizontal speed of the moving wall ω_{wall} and the LMS output signal ω^m, according to the following equation: $Std_{error} = std(\omega_{wall} - \omega^m)$. For each direction, the refresh rate $f_{refresh}$ was defined as the number of new motion measurements per second among the LMS of the specific direction: a new measurement occurs when a contrast

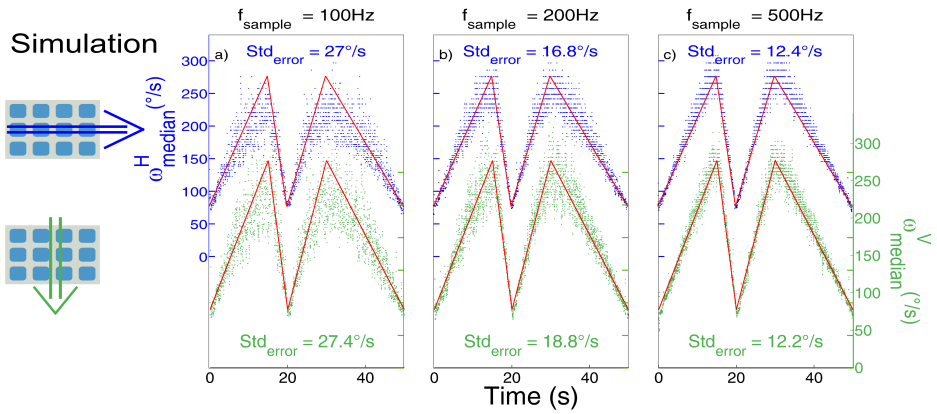

Figure 3. a-b-c) Simulated dynamic responses of the median angular speed of the visual motion sensor for three sampling rates for a horizontal translation (blue dots) and a vertical translation (green dots) in front of the textured wall moving according to a triangular law (red) (angular speed ranging from 75°/s to 275°/s with different slopes). In any case, the angular speed was measured thanks to a linear interpolation and faithfully obeyed the triangular law imposed to the moving wall. As expected, the accuracy of the measured angular speed (ω^H_{median}, ω^V_{median}) increases with the sampling rate. The dispersion was low enough ($Std_{error} < 19^o/s$) at 200Hz which is a good trade-off between accuracy and computational resources.

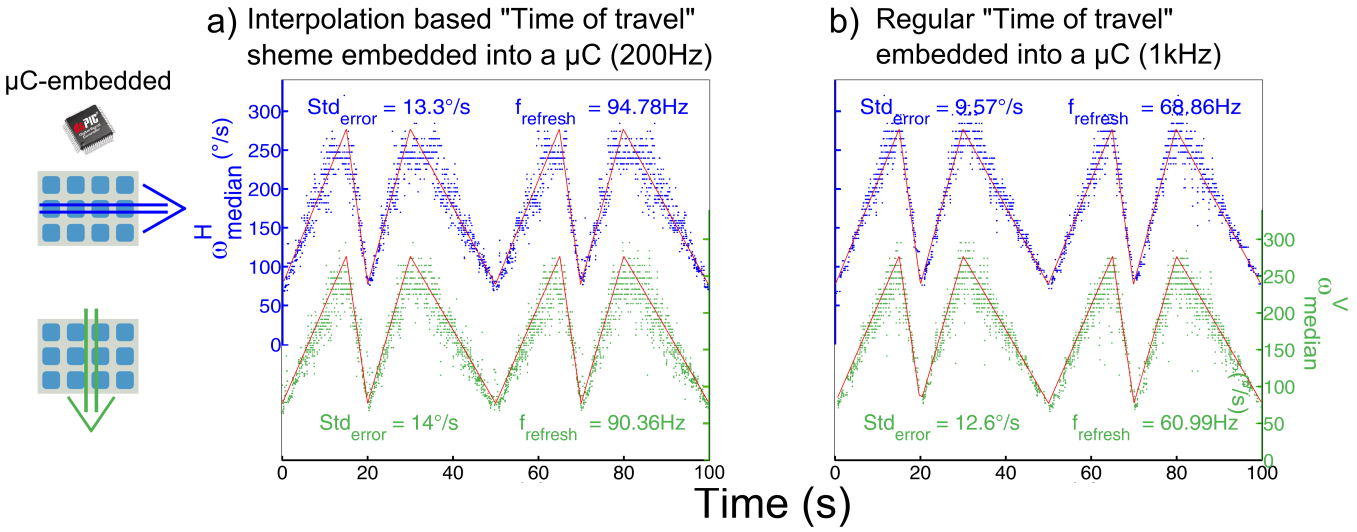

Figure 4. a) μC-embedded dynamic response of the median angular speed of the visual motion sensor at $f_{sample} = 200Hz$ measured thanks to a linear interpolation for a horizontal translation (blue dots) and a vertical translation (green dots) of the moving wall. The visual motion sensor yields at its output an accurate ($Std_{error} < 15^o/s$) and highly refreshed (nearly up to 100Hz) angular speed measurement (ω^H_{median}, ω^V_{median}). b) μC-embedded dynamic response of the median angular speed of the visual motion sensor at $f_{sample} = 1kHz$ measured thanks to the regular "time of travel" scheme. The refresh rate, which depends on the number of fused LMS, was greater for the horizontal motion than for the vertical motion as the median values were computed from 9 and 8 LMSs respectively.

transition is detected by one pixel and then by the second pixel with a time lag Δt in our measurement range, corresponding to an angular speed in the $[30^o/s, 350^o/s]$ range.

In order to determine the best trade-off between accuracy and computational load, a first set of experiments has been conducted in simulation using photoreceptor signals acquired at 3 different sampling rate frequencies (100, 200 and 500Hz) for a horizontal and a vertical motion. Then, the whole processing has been embedded into a dsPIC33FJ128GP804 microcontroller with a 200Hz sampling frequency.

A. Simulation of the interpolation based "Time of travel"

The interpolated algorithm presented in Fig. 2 was tested offline with three sampling rates (f_{sample}) on visual signals coming from the APIS retina. As we can see in the Fig. 3, the simulated responses of the horizontal and vertical angular speed measurements (ω^H_{median}, blue dots; ω^V_{median}, green dots) faithfully obeyed the triangular law imposed to the moving wall: the dispersion decreased with the sampling rate (from $Std_{error} = 27^o/s$ at 100Hz to $Std_{error} = 12^o/s$ at 500Hz). The simulated new sheme featured good performances at 200Hz which is the best trade-off between accuracy (dispersion lower than $19^o/s$) and limited computational load.

B. Interpolation based "Time of travel" embedded into a μC

A full duplex link between the UART peripheral of the μC and the computer serial port allowed us to log data from the VMS on a host computer. As shown in figure 4, the experimental measured median angular speed was highly refreshed and faithfully obeyed the triangular law imposed

to the moving wall ($Std_{error} < 15^o/s$). This processing accounts for only 10.5% in average of the processing time available at a sampling frequency of 200Hz (peak value:16%). In comparison, the same processing embedded into the µC at 1kHz requires 44.2% in average (peak value:71%) of the processing available. Although the processing is more than 4 times less costly at 200Hz than 1kHz, we can see that the accuracy (Std_{error}) of the data is experimentally only slightly better at 1kHz which proves that linearly interpolating the photoreceptors signals sampled at 200Hz is a really interesting trade-off between computational load and accuracy.

IV. Conclusion

In this study, the dynamic characteristics of a new optimized implementation of the "time of travel" scheme was tested indoors on a natural colored scene under natural light conditions. The results obtained here show that by linearly interpolating the photoreceptor signals sampled at 200Hz, we can greatly increase by at least 4 times the number of Local Motion Sensors that can be embedded in a small and lightweight microcontroller. This allowed us to compute all the possible LMSs from a 4x3 bio-inspired auto-adaptive pixel array in the 4 main directions. The overall Visual Motion Sensor (VMS) yields a median horizontal and vertical values (ω^H_{median} and ω^V_{median} respectively) which were found to be accurate and frequently refreshed. This VMS constitutes a good trade-off between the need for reliable and lightweight visual motion sensors matching the drastically limited payload of the Micro Aerial Vehicles.

As only 10.5% of the processing time available was used to process the angular speed of a small matrix of 12 pixels (4x3 pixel), this optimized implementation could be used to implement more LMSs into such tiny µC and therefore process the optic flow from 2D retinas having about 50 pixels. In a near future, this new visual motion sensor could be implemented on Micro Aerial Vehicles to process the local optic flow in several regions of the Field of View allowing them to fly autonomously in natural environments and perform complex tasks such as collision avoidance, automatic take-off and landing [10], [6]...

Acknowledgment

We are very grateful to M. Boyron for his help with the electronic design, Y. Luparini and J. Diperi for the mechanical design, G. Sabiron and N. Leroux for their help in the improvement of the processing. We thank R. Brinkworth and D. O'Carroll (Adelaide Uni., Australia) for kindly making their High Dynamic Range panoramic images available to us. This research was supported by CNRS Institutes (Life Science; Information Science; Engineering Science and Technology), Aix-Marseille University, the French National Research Agency (ANR) (EVA project under ANR-ContInt grant number ANR608-CORD-007-04), and by European Commission via the CURVACE project. The CURVACE project acknowledges the financial support of the European Commission's Future and Emerging Programme for Research , under FET-Open grant number: 237940.

References

[1] F. Aubépart, M. Ménouni, T. Loubignac, B. Dinkelspieler, and N. Franceschini. Capteur de flux optique basé sur une rétine intégrée et un FPGA. In *Colloque Interdisciplinaire en Instrumentation*, pages 508–520, Nancy, France, 2007. Paris: Hermes Science Publications.

[2] A. Beyeler, J-C. Zufferey, and D. Floreano. optiPilot: control of take-off and landing using optic flow. In *European Micro Aerial Vehicle Conference (EMAV)*, Delft, Netherlands, September 2009.

[3] C. Blanes. *Appareil visuel elementaire pour la navigation a vue d'un robot mobile autonome*. Master thesis in Neurosciences (DEA in French), advisor N. Franceschini, Neurosciences, Univ. Aix-Marseille II, Marseille, 1986.

[4] C. Blanes. *Guidage visuel d'un robot mobile autonome d'inspiration biologique 2nde Partie*. PhD thesis, advisor N. Franceschini, Institut National Polytechnique de Grenoble (INP Grenoble), 1991.

[5] T. Delbrück and C. A. Mead. Adaptive photoreceptor with wide dynamic range. In *IEEE International Symposium on Circuits and Systems (ISCAS)*, volume 4, pages 339–342, London, England, June 1994.

[6] F. Expert and F. Ruffier. Controlling docking, altitude and speed in a circular high-roofed tunnel thanks to the optic flow. In *IEEE/RSJ International Conference on Intelligent Robots and Systems (IROS)*, Vilamoura, Portugal, (accepted) October 2012.

[7] F. Expert, S. Viollet, and F. Ruffier. Outdoor field performances of insect-based visual motion sensors. *Journal of Field Robotics*, 28 (4):529–541, 2011.

[8] N. Franceschini, J. M. Pichon, and C. Blanes. From insect vision to robot vision. *Philosophical Transactions of the Royal Society B: Biological Sciences*, 337 (1281):283–294, 1992.

[9] N. Franceschini, A. Riehl, and A. Le Nestour. Directionally selective motion detection by insect neurons. In D.G. Stavenga and R. Hardie, editors, *Facets of Vision*, pages 360–390. Berlin & New York, Springer, 1989.

[10] N. Franceschini, F. Ruffier, and J. Serres. A bio-inspired flying robot sheds light on insect piloting abilities. *Current Biology*, 17:329 – 335, 2007.

[11] R. R. Harrison and C. Koch. A robust analog VLSI motion sensor based on the visual system of the fly. *Autonomous robots*, 7(3):211–224, 1999.

[12] B. Hassenstein and W. Reichardt. Systemtheoretische Analyse der Zeit-, Reihenfolgen-, und Vorzeichenauswertung bei der Bewegungsperzeption des Rüsselkafers. *Chlorophanus. Zeitschrift für Naturforschung*, 11:513–524, 1956.

[13] B.K.P. Horn and B.G. Schunck. Determining optical flow. *Artificial Intelligence*, 17:185–204, 1981.

[14] B.D. Lucas and T. Kanade. An iterative image registration technique with an application to stereo vision. In *International Joint Conference on Artificial Intelligence (IJCAI)*, pages 674–679, Vancouver, Canada, August 1981.

[15] M. Pudas, A. Kruusing, S. Leppävuori, M. Boyron, S. Amic, S. Viollet, and N. Franceschini. A miniature bio-inspired optic flow sensor based on low temperature co-fired ceramics (LTCC) technology. *Sensors and Actuator A: Physical*, 133:88–95, 2007.

[16] F.L. Roubieu, F. Expert, M. Boyron, B.-J. Fuschlock, S. Viollet, and F. Ruffier. A novel 1-gram insect based device measuring visual motion along 5 optical directions. In *IEEE Sensors 2011 conference*, pages 687–690, Limerick, Ireland, October 2011.

[17] F. Ruffier and N. Franceschini. Optic flow regulation: the key to aircraft automatic guidance. *Robotics and Autonomous Systems*, 50(4):177 – 194, 2005.

[18] F. Ruffier, S. Viollet, S. Amic, and N. Franceschini. Bio-inspired optical flow circuits for the visual guidance of micro-air vehicles. In *IEEE International Symposium on Circuits and Systems (ISCAS)*, volume 3, pages 846–849, Bangkok, Thailand, May 2003.

[19] M.V. Srinivasan. An image-interpolation technique for the computation of optic flow and egomotion. *Biological Cybernetics*, 71 (5):401–415, 1994.

[20] S. Viollet, F. Ruffier, T. Ray, M. Ménouni, F. Aubépart, L. Kerhuel, and N. Franceschini. Characteristics of three miniature bio-inspired optic flow sensors in natural environments. In *IEEE International Conference on Sensor Technologies and Applications (SENSORCOMM)*, pages 51–55, Venice, Italy, July 2010.

[21] J-C. Zufferey and D. Floreano. Fly-inspired visual steering of ultralight indoor aircraft. *IEEE Transactions on Robotics*, 22(1):137–146, 2006.